


CLINICAL REPORT

Opitz GBBB syndrome with total anomalous pulmonary venous connection: A new *MID1* gene variant

Maryangel Perea-Cabrera¹ | Javier T. Granados-Riveron¹ | Begoña Segura-Stanford² | Liliana M. Moreno-Vargas³ | Diego Prada-Gracia³ | Mari C. Moran-Espinosa¹ | Julio Erdmenger² | Hector Diaz-Garcia¹ | Rocío Sánchez-Urbina^{1,4} 

¹Centro de Investigación en Malformaciones Congénitas, Hospital Infantil de México Federico Gómez, Mexico City, Mexico

²Departamento de Cardiología, Hospital Infantil de México Federico Gómez, Mexico City, Mexico

³Unidad de Investigación en Biología Computacional y Diseño de Fármacos, Hospital Infantil de México Federico Gómez, Ciudad de México, Mexico

⁴Escuela Superior de Medicina del Instituto Politécnico Nacional, Mexico City, Mexico

Correspondence

Rocío Sánchez-Urbina, Hospital Infantil de México Federico Gómez, Dr. Márquez #162 Col. Doctores, Alcaldía: Cuauhtémoc, Mexico City, C.P. 06720, Mexico.
Email: roci0404@gmail.com

Funding information

Hospital Infantil de México Federico Gómez, Grant/Award Number: HIM/2015/036; Programa Nacional de Posgrados de Calidad of CONACyT Mexico

Abstract

Background: Opitz GBBB syndrome (GBBB) is an X-linked disease characterized by midline defects, including congenital heart defects. We present our diagnostic approach to the identification of GBBB in a consanguineous family in which two males siblings were concordant for a total anomalous connection of pulmonary veins and minor facial dysmorphias.

Methods: Targeted exome sequencing analysis of a 380-gene panel associated with cardiovascular disease was performed on the proband. Interpretative analysis of the exome results was conducted, and 3D models of the protein changes were generated.

Results: We identified a NM_000381.4:c.608G>A;p.(Arg203Gln) change in *MID1*, affecting the conformation of the B-box 2 domain of the protein, with a zinc finger structure and associated protein interactions. This clinical phenotype is consistent with GBBB; however, the type of congenital heart disease observed in this case has not been previously reported.

Conclusion: A new likely pathogenic variant on *MID1* c.608G>A was found to be associated with Opitz GBBB syndrome.

KEYWORDS

congenital heart defects, Opitz GBBB syndrome, total anomalous pulmonary venous connection

1 | INTRODUCTION

Opitz GBBB syndrome (MIM #300000) is a Mendelian condition characterized by midline defects with significant variable expressivity (Meroni, 1993). Symptoms may include cerebellar hypoplasia, broad forehead, hypertelorism,

facial clefts, tracheoesophageal fistulas, hypospadias (Maia et al., 2017), and congenital heart disease (CHD) (Cheng et al., 2014) with or without intellectual disability (Mnayer et al., 2006). GBBB with X-linked inheritance is caused by mutations in the *MID1* gene on Xp22.2 (Fagerberg et al., 2014). The variable expressivity of GBBB can be

This is an open access article under the terms of the [Creative Commons Attribution-NonCommercial-NoDerivs](https://creativecommons.org/licenses/by-nc-nd/4.0/) License, which permits use and distribution in any medium, provided the original work is properly cited, the use is non-commercial and no modifications or adaptations are made.

© 2023 The Authors. *Molecular Genetics & Genomic Medicine* published by Wiley Periodicals LLC.

explained by its expression in the embryonic development of the craniofacial region, nervous system, gastrointestinal and urogenital systems (Dal Zotto et al., 1998), and by the large number of genes regulated by *MID1*.

In this report, we present the diagnostic approach of GBBB in a consanguineous Mexican family. Two siblings presented with a total anomalous pulmonary venous connection (TAPVC) and minor facial dysmorphias. The diagnosis of GBBB was established through exome sequencing analysis of the proband employing a panel of 380 genes associated with cardiovascular disease. The results showed a previously unreported missense variant, c.608G>A, in *MID1*. We created 3D models of the protein changes.

2 | MATERIALS AND METHODS

The proband was born from a consanguineous uncle-niece couple. The father was 31 years old (III3), mother was 25 years old (IV1), and both were healthy (Figure 1a). The proband (V5) was born at 39 weeks of gestation after a normal pregnancy and eutocic delivery. The birth weight was 3.8 kg (90th centile) and birth height was 53 cm (90th centile). Apgar score of 8–7 and Silverman Anderson score of 0. His psychomotor development was adequate, with self-head support at 3 months, sitting at 6 months, and standing at 11 months of age. At the age of 7 months, the proband was diagnosed with CHD type TAPVC (Figure 1g) and underwent cardiovascular surgical correction at 8 months of age. At the time of writing, he was 2 years 6 months old. Physical examination: weight of 13 kg (50th percentile), height of 90 cm (25th percentile), normal psychomotor development, a broad forehead, hypertelorism, a median scar on the thorax, a normal renal ultrasound, normal male genitalia with descended testicles, a well-positioned urinary meatus, and no other congenital anomaly. The brother of the proband (V4), at 2 years of age, had shown mild psychomotor developmental delay, weight of 8.55 kg (percentile <3), height of 76 cm (percentile <3), and CHD type TAPVC, diagnosed by echocardiogram at 9 months (Figure 1e,f). This was treated by cardiovascular surgery in our institution when he was 1 year old. However, he died at home at the age of 2 due to cardiopulmonary complications. All living siblings of the proband (V1, V2, and V3) were clinically evaluated, and medical records were reviewed.

2.1 | Whole-exome sequencing

Prior informed consent, a saliva sample of the proband was obtained and sent to Health in Code for processing in line with our in-house protocol ([https://www.ncbi.](https://www.ncbi.nlm.nih.gov/gtr/labs/320229/)

[nlm.nih.gov/gtr/labs/320229/](https://www.ncbi.nlm.nih.gov/gtr/labs/320229/)). After genomic DNA isolation, 10 ng of DNA was used for library construction, exon capture, and paired-end read sequencing using the SureSelect XT Library Prep Kit (Agilent) with enrichment using SureSelect XT Clinical Research Exome v.2 probes (Agilent) on an Illumina HiSeq 4000 (Illumina). A 380-gene panel associated with cardiovascular disease was analyzed on the Health in Code platform.

2.2 | Bioinformatics

FASTQ files containing the generated reads were aligned to the human reference genome (NCBI GRCh38/hg38 version) using BWA and BAM files, which were generated using Samtools. The Genome Aggregation Database (<https://gnomad.broadinstitute.org/>) was used to call sequence variants. Genetic variant annotations were implemented with wANNOVAR (<https://wannovar.wglab.org/>), considering intronic (splice and nonsplicing sites), exonic (synonymous, nonsynonymous, insertion, deletion, or stop functions), and 5- and 3-UTR regions. The variants identified in the proband that are not present in the general population were selected for further analysis to evaluate their pathogenicity using mutation taster (<https://www.mutationtaster.org/>), as were deleterious annotation of genetic variants using the neural networks (DANN) algorithm and fathmm v.2.3 (<http://fathmm.biocompute.org.uk/>). For the frequency of the variants (minor allele frequency [MAF]), we consulted data available in the 1000 Genomes Project (<https://www.genome.gov/27528684/1000-genomes-project>), the Single Nucleotide Polymorphism Database (dbSNP) (<http://www.ncbi.nlm.nih.gov/SNP>), and the (Exome Variant Server, NHLBI GO Exome Sequencing Project (ESP), n.d.) (<https://evs.gs.washington.edu/EVS/>).

The protein sequences of *MID1* for several animal species were obtained from the NCBI database (<https://www.ncbi.nlm.nih.gov/gene>): human (NP_001334662.1), mouse (NP_034927.2), cat (XP_004000308.1), cow (NP_001179751.1), sheep (XP_004021948.1), chicken (NP_989460.1), Amazon molly (XP_007557159), zebrafish (XP_002663478.1); and from Ensembl (<https://www.ensembl.org/>): chimpanzee (ENSPTRT00000077271.1), and wal-laby (ENSMEUG00000010101). These were compared to the human protein using a global alignment performed with Clustal Omega (<https://www.ebi.ac.uk/Tools/msa/clustalo/>).

2.3 | Sanger sequencing

The proband's genomic DNA (gDNA) was purified from epithelial oral cells using the Presto Buccal Swab gDNA

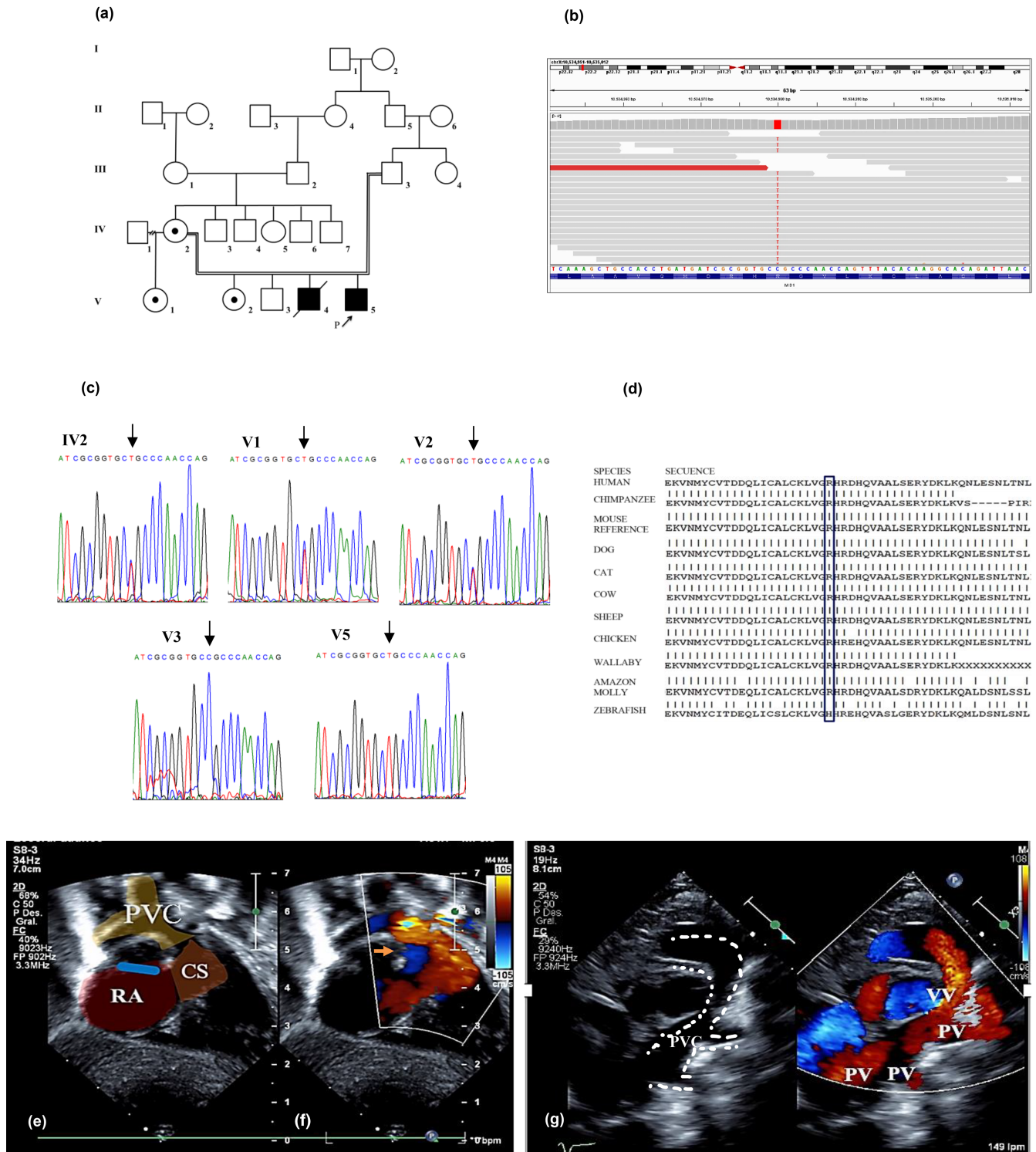


FIGURE 1 (a) Pedigree showing the consanguineous union between the parents of the proband. (b) Alignment of total exome reads spanning exon 2 of *MID1* gene, showing the C>T transition causing the Arg203Gln mutation in the patient. (c) Sanger sequencing trace showing the C>T hemizygous transition in the proband and the same heterozygous variant in IV1 and V3 hemizygous for C allele. (d) Global alignment of the *MID1* orthologs from several species showing high conservation of the arginine (R) residue. The zebrafish shows a histidine [H] residue and a charged polar amino acid. (e) Echocardiogram subject V4, prior to corrective surgery. Subcostal view visualizing the pulmonary veins collector (PVC) arriving at the dilated coronary sinus (CS). (f): Subcostal view visualizing both atria (RA, LA) and atrial septal defect (arrow) with right to left shunt. (g) Echocardiogram of the propositus (V5) prior to corrective surgery, suprasternal view showing the pulmonary veins (PV) reaching the vertical vein (VV) and pulmonary veins collector (PVC) is observed (dotted line).

Extraction Kit (Geneaid Biotech Ltd). The gDNA of his siblings and mother was isolated from blood using the Genra Puregene Blood Kit (Qiagen). The primers for the polymerase chain reaction (PCR) amplicon for Sanger sequencing (forward; 5'-GTCCTCTGCCAGTTTTGTGAC-3', and reverse; 5'-CCTTACCTGCCATGTAGC-3') were designed in Primer3web (<https://primer3.ut.ee/>). PCR amplifications were carried out with GoTaq® Green Master Mix (Promega) following the manufacturer's instructions. The PCR conditions consisted of 1 cycle of preheating at 95°C/3 min; 35 cycles of amplification; denaturation at 95°C/30s; annealing at 59°C/20s; extension at 70°C/20s; and a final extension at 70°C/5 min. PCR products were run in agarose gel at 2.5% and purified from gel bands using the QIAquick PCR Purification Kit (Qiagen). Sanger reactions were carried out on 50 ng of purified PCR-amplified DNA using the BigDye Terminator v.3.1 Kit (Thermo Fisher Scientific) and then were purified in turn using Centri-Sep Spin Columns (Thermo Fisher) according to the manufacturer's instructions. Finally, the Sanger products were subjected to capillary electrophoresis in a 310 Genetic Analyzer (Thermo Fisher). Electropherograms were analyzed using MEGA software, v. 10.0.5 (Penn State).

2.4 | Molecular modeling of the E3 ubiquitin-protein ligase Midline-1

The 667 amino acid sequence of the E3 ubiquitin-protein ligase Midline-1 (accession number NP_001334662.1) was obtained from the NCBI protein reference database (<https://www.ncbi.nlm.nih.gov/protein>). To generate a model of the protein encoded by the *MID1* gene, we used two independent strategies and then chose the consensus model. For the first strategy, we used an assembly of large rigid fragments obtained from similar structures aligned using their primary and secondary sequences. Using this methodology, fragments of the peptide skeletons of known structures are cut and pasted (the Swiss-Model) (Waterhouse et al., 2018). For the second strategy, we used modeling satisfying the constraints of the molecules extracted from databases and similarly aligned structures. This method produces a set of structures for the sequence compatible with the restrictions observed in the templates (Modeler) (Eswar et al., 2006). A structure predicted by AlphaFold Monomer v.2.0 was used to corroborate the folding of the models obtained (data not shown) (Jumper et al., 2021). To generate a model of the p. Arg203Gln variant, we used the structural data of the B-box-2 domain, which was obtained from the Protein Data Bank (ID PDB: 2JUN). The altered form of p.Arg203Gln identified in GBBB was found in this domain.

2.5 | Geometric optimization of the proposed models

Once the models were prepared, hydrogen atoms were added, and side-chain orientations were optimized through the steepest descent method of energy minimization using a CHARMM36 force field (Huang et al., 2017) in a TIP3P water box (Jorgensen et al., 1983).

2.6 | Stereochemical quality evaluation of the models

Coordinate files of the models were sent to MolProbity (Chen et al., 2010) to produce a Ramachandran plot (with ϕ and ψ angles) that reflected the polypeptide chain distortion in the restricted region. The quality of the models was further validated using ProQ3/ProQ3D (Uziela et al., 2017) and QMEAN (Benkert et al., 2009).

3 | RESULTS

Clinical evaluation of the propositus (V5) and details of the family history revealed minor facial dysmorphias and TAVPC with an apparent autosomal recessive inheritance pattern for CHD. Genomic analysis showed a hemizygous variant in *MID1* (NCBI Reference Sequence: NM_000381.4) (www.ncbi.nlm.nih.gov/gene), consisting of a c.608G>A missense variant (Figure 1b). This was also present in a heterozygous state in the mother (III1) and sisters (V1, V2) (Figure 1c). Clinical and cardiological evaluations of the siblings (V1, V2, and V3) of the propositus found no perinatal diseases, normal psychomotor development and growth, no cardiovascular defects, and absence of facial dysmorphism or other physical anomalies or diseases. Therefore, the clinical familial presentation and the determination of the heterozygous variant state of the siblings of the propositus established an X-linked inheritance pattern (Figure 1a,c) which demonstrates a PP4 pathogenicity criterion of the variant c.608G>A for GBBB (Richards, et al., 2015). Therefore, the family was provided with genetic counseling for an X-linked disease, where the mother and sisters are heterozygous for the mutation with a 50% risk of presenting the disease in their male offspring and 50% of carriers of the c.608G>A mutation in daughters.

For the study of the propositus (V5), we employed a Health in Code panel of 380 genes known to cause cardiovascular disease. Within these genes, only one previously unreported missense variant was found in *MID1* that caused a change in the protein by substitution of Arg203Gln. This position comprises a part of the domain

B-Box type 2, located in a hot spot, considered a critical and well-established functional domain (zinc finger of the protein). MID1 has 2 B-Box domains of type 1 and type 2 (B1B2) in tandem. A high-resolution structure of the individual domains (B-Box type 1 and B-Box type 2) showed that both domains coordinate two zinc atoms in a cross-brace fashion and adopt $\beta\beta\alpha$ RING-like folds (Mnayer et al., 2006). The 2 B-Box domains form an interface composed of residues located on the structured loop consisting of the two antiparallel β -strands. The surface of the interface is 188 \AA^2 , representing 17% of the total surface. Thermodynamic data reveal a stable interaction between the B-Box type 1 and B-Box type 2 domains, since according to the globular structure, the T_m of the tandem B-Box domain (59°C) is higher than that of the individual domains (Tao et al., 2008). Mutations within either the B-Box 1 or the B-Box 2 domains (ΔCys137 , Cys142Ser , Cys145Tyr , Cys195Phe , Ala130Val , and Ala130Ser) of MID1 have been found in patients with GBBB (Table 1) (Cox et al., 2000; Ferrentino et al., 2007; Pinson et al., 2004; So et al., 2005). Such mutations are believed to result in the loss of MID1 function. The change in the 203 position of the protein is linked to the alteration of the chemical environment generated in the region of one of the zinc fingers present in the structure of the protein, probably preventing the union of the metal, essential to exert the function of domain B-Box 2, and the stabilization of the tandem domain interface (Figure 2). Therefore, according to this information, the c.608G>A variant was assigned the PP3 pathogenicity criterion (Richards et al., 2015).

There is evidence of the regulation of B-Box 1 by B-Box 2. Midline-1 (MID1) is required in the process of proteasomal degradation of the catalytic subunit of protein phosphatase 2A (PP2Ac). This function of MID1 is facilitated by the direct binding of Alpha4, a regulatory subunit of PP2Ac, to B-Box1, while the presence of the B-Box2 domain of MID1 does impact this interaction and the affinity between B-Box1 and Alpha4. The importance of both B-Boxes is evident, and when this interaction is destabilized, the result is the loss of MID1 function (Trochenbacher et al., 2001).

As described above, the c.608G>A variant is located within the B-Box 2 domain encoding segment, allowing the PM1 pathogenicity criterion to be assigned as it is in a functional domain (Richards et al., 2015).

This variant has not been previously reported in GBBB patients (Table 1). The analysis of the predictors used to determine the effect of the variant resulted in a mutation taster value of 1; DANN: 0.999383; FTHMM MKL coding: 0.93828 and FTHMM MKL noncoding: 0.98801, all suggesting a pathogenic effect of the variant. The c.608G>A change in *MID1* has been found in only two alleles of 178,654 analyzed in heterozygous state in two

Latina women, with no occurrences in other populations (Auton et al., 2015; gnomAD, Genome Aggregation Database, 2021) or the Exome Variant Server (Exome Variant Server, NHLBI GO Exome Sequencing Project (ESP), n.d.), this gives us a pathogenicity criterion PM2 (Richards, S., et al., 2015). Additionally, the global alignment of *MID1* orthologs from several species revealed a high degree of conservation of the wild-type arginine (R) residue, while zebrafish shows a histidine [H] residue and a charged polar amino acid (Figure 1d).

4 | DISCUSSION

The highly variable expressivity of GBBB described in multiple studies (Table 1) was corroborated by the clinical presentation of the patient in this case (V5), who showed minor facial dysmorphism in the form of a wide forehead and hypertelorism. Both dysmorphias are frequent symptoms of GBBB. Hypertelorism is found in 100% of affected males and 50% of female carriers (Table 1). However, female carriers in the family of our study did not show hypertelorism or other facial or cardiovascular disorders. Although there are no established clinical criteria for the diagnosis of patients with GBBB, major and minor clinical features are considered in the pathology (Meroni, 1993). In the propositus (V5), there were two major features (hypertelorism and family history) and two minor traits (broad forehead and CHD). The type of CHD observed, which was concordant between the two brothers (V4 and V5), has not been previously reported in GBBB. The most frequent type of CHD described in the literature is ventricular septal defects (Table 1). However, TACVP is one of the most common complex forms of CHD in the Mexican population (Evans et al., 2015); therefore, we cannot rule out a potential predisposition to this type of CHD due to the patient's ethnicity. We propose that patients with these clinical characteristics, including TACVP, and family history consistent with an X-linked inheritance pattern, should be evaluated for GBBB.

4.1 | MID1

The *MID1* codes for a protein known as Midline-1 (Mid1) comprised 667 amino acids, which form multiprotein complexes. The main function of Mid1 is the formation of homodimers for ubiquitination with microtubules (Wright et al., 2016). It is expressed in 27 types of human tissue, including that of the heart. Pathogenic changes in the *MID1* gene and its loss of function have been reported (Aranda-Orgillés et al., 2008; Liu et al., 2001; Massiah et al., 2006; Short et al., 2002). We found an amino acid

TABLE 1 Reported mutations and clinical description of patients.

Author	Mutation	Phenotype not specified	Hypertelorism	Cleft lip and/or palate	Tracheoesophageal fistula	Anal atresia	Hypospadias
So et al. (2005)	c.884T>C	-	X	X	-	-	X
	c.1545_1546delGA	-	X	X	X	X	X
	c.1171_1173delTCT	-	X	X	-	X	X
	c.1656G>A	-	X	X	-	X	X
	p.W552X	X	-	-	-	-	-
	c.IVS3_16>T	-	X	X	-	-	X
	c.1445_1446insAAA	-	X	-	-	-	X
	c.1313_1316delTGAT	-	X	X	-	-	-
	c.IVS7+1G>A	-	X	X	-	-	X
	c.IVS7_8_1447ins20pb	-	X	X	-	-	X
	c.829C>T	-	X	X	-	-	X
Zhang et al. (2011)	c.712G>T	-	X	-	-	-	X
	c.1230G>A	-	X	-	-	-	X
	c.1284T>G	-	X	-	-	-	X
	1679A>G	-	X	-	-	-	X
Cheng et al. (2014)	c.1798insC	-	X	X	-	-	X
	c.del3UTR	X	-	-	-	-	-
Cho et al. (2006)	c.1798insC	-	X	-	X	-	X
Ferrentino et al. (2007)	c.712G>T	-	X	-	-	-	X
	c.434G>A	X	X	-	-	-	-
	c.1793delC	X	X	-	-	-	-
	c.1285+1G>T	X	X	-	-	-	-
	c.397_401delACCTG	X	X	-	-	-	-
	c.1832A>G	X	X	-	-	-	-
	c.819_829del11	X	X	-	-	-	-
	c.864+1G>T	X	X	-	-	-	-
	c.388G>A	X	X	-	-	-	-
	c.1141+2T>C	X	X	-	-	-	-
	c.1573C>T	X	X	-	-	-	-
	c.1856_1858delATG	X	X	-	-	-	-
	c.1957G>A	X	X	-	-	-	-
	c.1611_1612insTGAT	X	X	-	-	-	-
	c.950_951insA	X	X	-	-	-	-
	c.1108A>G	X	X	-	-	-	-
	c.389A>T	X	X	-	-	-	-
	c.561T>A	X	X	-	-	-	-
	c.1605_1606insGTTT	X	X	-	-	-	-
	c.1594G>A	X	X	-	-	-	-
	c.1452_1455delACCA	X	X	-	-	-	-
	c.430G>T	X	X	-	-	-	-
	c.425G>C	X	X	-	-	-	-
c.1491_1533dup43	X	X	-	-	-	-	
c.1663A>G	X	X	-	-	-	-	

TABLE 1 (Continued)

Author	Mutation	Phenotype not specified	Hypertelorism	Cleft lip and/or palate	Tracheoesophageal fistula	Anal atresia	Hypospadias
Cox et al. (2000), Preiksaitiene et al. (2015)	c.1102C>T	-	X	X	X	-	X
	c.1877T>C	-	X	X	-	-	X
	c.1051delC	-	X	X	-	-	-
	c.1483C>T	-	X	-	X	-	X
	c.1402C>T	-	X	-	X	-	X
	c.221_252del	-	X	-	X	-	-
	c.343G>T	-	X	X	X	-	X
De Falco et al. (2003)	c.1387G>T	-	X	X	X	-	X
	c.1331insA	-	X	X	X	-	X
	c.1483C>T	-	X	X	X	X	X
	c.757G>C	-	X	X	X	-	X
	c.1286G>A	-	X	-	-	-	X
	c.1551insGTCCAC	-	X	-	X	X	X
	c.584G>T	-	X	-	X	X	X
	c.1039C>T	-	X	-	X	X	X
	c.1106_1107delAG	-	X	X	X	-	X
c.1267G>T	-	X	-	X	-	-	
Fontanella et al. (2008)	c.571T>A	-	X	X	-	-	X
	C.584G>T	-	X	-	X	X	X
	c.606delG	-	X	-	X	-	X
Hüning et al. (2013)	c.221_252dup	-	X	-	-	-	-
Mnayer et al. (2006)	c.1322C>T	-	X	-	X	-	X
Pinson et al. (2004)	c.1354G>A	-	X	-	-	-	X
	c.829 C>T	-	X	X	X	-	X
	c.1285_1289delGAGT	-	X	-	X	-	X
	c.1447insAACA	-	X	-	X	X	X
	c.1483C>T	-	X	X	-	-	X
c.403_411delTCACTTG TG	-	X	-	-	X	X	
Ruiter et al. (2010)	c.1108A>G	-	X	-	-	-	-
Shaw et al. (2006)	c.1483	-	X	X	-	-	X
Taylor et al. (2015)	c.1798dupC	-	X	-	X	X	X
Present report	c.688C>T	-	X	-	-	-	-

Abbreviations: ASD, atrial septal defect; BSVC, bilateral superior vena cava; CA, coarctation of aorta; DORV, double outlet right ventricle; HLH, hypoplastic left heart; NS, not specified; PAH, pulmonary artery hypoplasia; PAS, pulmonary artery stenosis; PDA, patent ductus arteriosus; SVC, superior vena cava; TAPVC, total anomalous pulmonary venous connection; VSD, ventricular septal defect.

substitution at position 203 in the protein with the development of GBBB. In this respect, eight natural variants of the Mid1 protein have been reported in the literature at positions 266, 295, 391, 392, 438, 534, 536, and 626 (Figure 2a) (<https://www.uniprot.org/uniprot/O15344>). The effects of this would be linked to alterations in the

chemical environment generated in the region of one of the three zinc fingers present in the structure of the protein, which would prevent the zinc union essential to the function of the B-Box 2 domain (Figure 2b). If a change occurred between amino acids of different polarity in the side chain of residue 203, close to a metal-binding site

Intellectual disability	Low auricular implantation	Auricular dysplasia	Widow's peak	Swallowing/ chewing disorders	Renal disease	Polyhydramnios	Mother with hypertelorism	Congenital heart disease
-	X	X	X	X	-	-	-	-
-	X	X	-	-	-	-	-	PAS, ASD
-	X	X	X	X	-	-	-	ASD, CA, VSD
X	-	X	X	X	X	-	-	VSD
X	-	X	X	X	-	-	-	VSD, PAS
X	-	X		X	-	-	-	-
X	-	X	X	X	X	-	-	-
-	-	-	-	-	-	-	-	-
-	-	-	-	-	-	-	-	-
-	X	-	-	-	-	X	-	-
-	-	-	-	-	-	X	-	SVC, VSD
-	-	-	-	-	-	-	-	-
-	-	-	-	-	-	-	-	-
X	-	-	-	-	-	-	-	-
-	-	-	-	-	-	X	-	-
X	X	-	-	-	-	-	-	PDA
-	X	-	-	-	-	-	-	-
X	-	-	-	-	-	-	-	-
X	-	-	-	-	-	-	-	-
X	-	-	-	-	-	-	-	-
-	-	-	-	X	-	-	X	-
-	-	X	X	-	-	-	-	-
-	X	-	-	-	X	-	X	-
X	X	-	-	-	-	-	-	-
X	X	-	X	-	-	-	X	NS
-	-	-	-	-	X	-	-	-
X	X	-	-	X	-	-	-	VSD
-	X	-	-	X	-	-	-	-
-	-	-	-	-	-	-	-	-
X	-	-	-	-	-	-	X	BSVC
-	-	-	-	-	-	-	-	-
-	-	-	-	-	-	-	-	TAPVC

(204) of the zinc finger at positions 172–212 (Figure 2c), it could directly affect the structure. The alteration of the chemical environment necessary to coordinate the zinc ions in that region would precipitate this. Since zinc fingers normally function as interaction modules linking genetic material, proteins, peptides, or small molecules,

these proteins often play essential roles in the stabilization of the quaternary structure or the induction of an active conformation. The destabilization of the quaternary structure can impede the correct formation of the functional structure of the Mid1 zinc finger and of its active conformations. A change in the interaction distances of

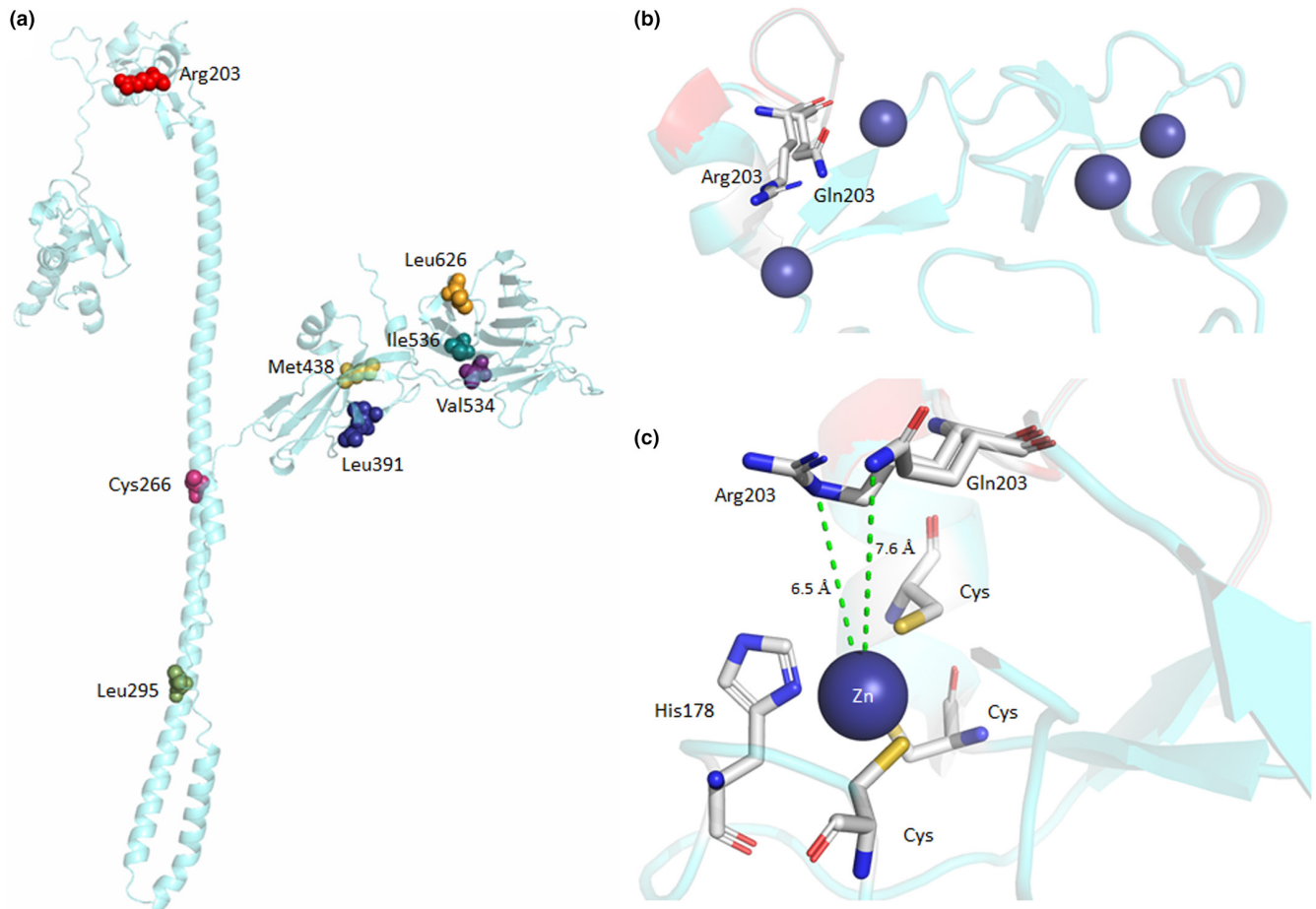


FIGURE 2 (a) The three-dimensional structure of E3 ubiquitin-protein ligase Midline-1, as determined by molecular modeling and the spatial locations of surface mutations. Eight natural variants of the protein have been reported in the literature, with mutations at positions 266 (C→R, in warm pink), 295 (L→P, in olive), 391, and 392 (LC→R, in deep blue), 438 (missing, in yellow), 534 (V→VFIDSGRHL, in violet purple), 536 (I→T, in deep teal), and 626 (L→P, in orange). The position corresponding to Arg 203 is shown in red. (b) Alignment of the B-box 2 domain of the wild-type E3 ubiquitin-protein ligase Midline-1 (cyan) and the mutant protein (red). Located in this domain is a zinc finger (at positions 172–212, which numbers correspond to those in the PDB file 2JUN), consisting of an alpha-helix and an antiparallel beta-sheet. (c) The zinc ion (deep blue) is coordinated by histidine 178 (H178) and three cysteines (C175, C195, and C198). The mutation of a charged amino acid (Arg, R) by an amidic amino acid (Gln, Q) implies both the shortening of the length of the side-chain and changes in the physicochemical and acid–base properties of the residue. The mutation by Q necessarily implies the destabilization of the zinc finger region, mainly in its interaction with the imidazole ring of H178. The modification of the chemical environment generates structural destabilization. The main detrimental effect of this is a decrease in the specificity of the zinc finger. A more long-distance effect that may result is the abolition of molecular recognition by other biomolecules.

the amino group in Arg (6.5 Å) was observed in the mutant form (7.6 Å).

Based on the above information, we interpreted the c.608G>A variant found in the present study is likely pathogenic due to a combination of two moderate and two supporting criteria for pathogenicity (Richards, S., et al., 2015). These were (a) its localization within the B-Box type 2 domain, a critical and well-established functional domain (zinc finger of the protein) (PM1) and a hot spot of the protein; (b) the frequency of the allele in the general population is 0.001% (PM2); (c) the deleterious effect of the variant in the protein by computational analysis (PP3), and (d) the inheritance pattern of the variant as

well as the phenotype observed in the family studied (PP4) (Richards et al., 2015).

4.2 | Conclusion

A new likely pathogenic variant in *MIDI1* c.608G>A was found to be associated with Opitz GBBB syndrome.

AUTHOR CONTRIBUTIONS

Rocío Sánchez-Urbina conceived the research, acquired funding, carried out the analyses to obtain results, collaborated with the assembly of the first draft of the manuscript, and

incorporated the suggestions of co-authors. Javier T. Granados-Riveron designed the project and interpreted the data. Maryangel Perea-Cabrera, Begoña Segura-Stanford, and Julio Erdmenger performed the clinical and cardiological evaluation of the proband and sibling affected with TAPVC. Maryangel Perea-Cabrera, Hector Diaz-Garcia, and Moran-Espinoza MC carried out experimental work and developed data analysis and interpretation. Maryangel Perea-Cabrera and Hector Diaz-Garcia developed the first draft manuscript. Liliana M Moreno-Vargas and Diego Prada-Gracia developed experimental design and data analyses of molecular modeling of E3 ubiquitin-protein ligase Midline-1. All authors collaborated on the writing and have read and approved the final manuscript.

ACKNOWLEDGEMENTS

The authors would like to thank the Research Unit of the Hospital Infantil de Mexico Federico Gómez for supporting this study. The authors would like to thank the patient's families for their support in this study.

FUNDING INFORMATION

This study was funded by an internal grant at Hospital Infantil de Mexico Federico Gómez, Mexico (grant number: HIM/2015/036). The author Maryangel Perea-Cabrera acknowledges the support of the Programa Nacional de Posgrados de Calidad of CONACyT Mexico.

CONFLICT OF INTEREST STATEMENT

The authors have no conflicts of interest to disclose. No honorarium, payment, or grant was given to any author to produce this study.


DATA AVAILABILITY STATEMENT

The data that support the findings of this study are available from the corresponding author upon reasonable request.

ETHICS STATEMENT

This study was conducted in accordance with the tenets of the 2013 version of the Declaration of Helsinki. The study was approved by the institutional review board (Ethics Committee) of Hospital Infantil de Mexico Federico Gómez (HIM/2015/036, February 10th, 2015). Signed statements of informed consent to participation and publication were obtained from the patient and his parents.

ORCID

Rocío Sánchez-Urbina  <https://orcid.org/0000-0001-8018-7749>

REFERENCES

Aranda-Orgillés, B., Trockenbacher, A., Winter, J., Aigner, J., Köhler, A., Jastrzebska, E., Stahl, J., Müller, E.-C., Otto, A., Wanker, E.

- E., Schneider, R., & Schweiger, S. (2008). The Opitz syndrome gene product MID1 assembles a microtubule-associated ribonucleoprotein complex. *Human Genetics*, *123*(2), 163–176. <https://doi.org/10.1007/s00439-007-0456-6>
- Auton, A., Brooks, L. D., Durbin, R. M., Garrison, E. P., Kang, H. M., Korbel, J. O., Marchini, J. L., McCarthy, S., McVean, G. A., & Abecasis, G. R. (2015). A global reference for human genetic variation. *Nature*, *526*(7571), 68–74. <https://doi.org/10.1038/nature15393>
- Benkert, P., Künzli, M., & Schwede, T. (2009). QMEAN server for protein model quality estimation. *Nucleic Acids Research*, *37*(Web Server issue), W510–W514. <https://doi.org/10.1093/nar/gkp322>
- Chen, V. B., Arendall, W. B., 3rd, Headd, J. J., Keedy, D. A., Immormino, R. M., Kapral, G. J., Murray, L. W., Richardson, J. S., & Richardson, D. C. (2010). MolProbity: All-atom structure validation for macromolecular crystallography. *Acta Crystallographica. Section D, Biological Crystallography*, *66*(Pt 1), 12–21. <https://doi.org/10.1107/S0907444909042073>
- Cheng, Y. K., Huang, J., Law, K. M., Chan, Y. M., Leung, T. Y., & Choy, K. W. (2014). Prenatal diagnosis of maternally inherited X-linked Opitz G/BBB syndrome by chromosomal microarray in a fetus with complex congenital heart disease. *Clinica Chimica Acta*, *436*, 140–142. <https://doi.org/10.1016/j.cca.2014.05.006>
- Cho, H. J., Shin, M. Y., Ahn, K. M., Lee, S. I., Kim, H. J., Ki, C. S., & Kim, J. W. (2006). X-linked Opitz G/BBB syndrome: Identification of a novel mutation and prenatal diagnosis in a Korean family. *Journal of Korean Medical Science*, *21*(5), 790–793. <https://doi.org/10.3346/jkms.2006.21.5.790>
- Cox, T. C., Allen, L. R., Cox, L. L., Hopwood, B., Goodwin, B., Haan, E., & Suthers, G. K. (2000). New mutations in MID1 provide support for loss of function as the cause of X-linked Opitz syndrome. *Human Molecular Genetics*, *9*(17), 2553–2562. <https://doi.org/10.1093/hmg/9.17.2553>
- Dal Zotto, L., Quaderi, N. A., Elliott, R., Lingerfelter, P. A., Carrel, L., Valsecchi, V., Montini, E., Yen, C. H., Chapman, V., Kalcheva, I., Arrigo, G., Zuffardi, O., Thomas, S., Willard, H. F., Ballabio, A., Disteche, C. M., & Rugarli, E. I. (1998). The mouse Mid1 gene: Implications for the pathogenesis of Opitz syndrome and the evolution of the mammalian pseudoautosomal region. *Human Molecular Genetics*, *7*(3), 489–499. <https://doi.org/10.1093/hmg/7.3.489>
- De Falco, F., Cainarca, S., Andolfi, G., Ferrentino, R., Berti, C., Rodríguez Criado, G., Rittinger, O., Dennis, N., Odent, S., Rastogi, A., Liebelt, J., Chitayat, D., Winter, R., Jawanda, H., Ballabio, A., Franco, B., & Meroni, G. (2003). X-linked Opitz syndrome: Novel mutations in the MID1 gene and redefinition of the clinical spectrum. *American Journal of Medical Genetics. Part A*, *120A*(2), 222–228. <https://doi.org/10.1002/ajmg.a.10265>
- Eswar, N., Webb, B., Marti-Renom, M. A., Madhusudhan, M. S., Eramian, D., Shen, M. Y., Pieper, U., & Sali, A. (2006). Comparative protein structure modeling using Modeller. *Curr Protoc Bioinformatics*, Chapter 5, Unit-5.6. <https://doi.org/10.1002/0471250953.bi0506s15>
- Evans, W. N., Acherman, R. J., Ciccolo, M. L., Castillo, W. J., & Restrepo, H. (2015). An increased incidence of total anomalous pulmonary venous connection among Hispanics in southern Nevada. *Congenital Heart Disease*, *10*(2), 137–141. <https://doi.org/10.1111/chd.12199>
- Exome Variant Server, NHLBI GO Exome Sequencing Project (ESP). <http://evs.gs.washington.edu/EVS/>

- Fagerberg, L., Hallström, B. M., Oksvold, P., Kampf, C., Djureinovic, D., Odeberg, J., & Uhlén, M. (2014). Analysis of the human tissue-specific expression by genome-wide integration of transcriptomics and antibody-based proteomics. *Molecular & Cellular Proteomics*, 13(2), 397–406. <https://doi.org/10.1074/mcp.M113.035600>
- Ferrentino, R., Bassi, M. T., Chitayat, D., Tabolacci, E., & Meroni, G. (2007). MID1 mutation screening in a large cohort of Opitz G/BBB syndrome patients: Twenty-nine novel mutations identified. *Human Mutation*, 28(2), 206–207. <https://doi.org/10.1002/humu.9480>
- Fontanella, B., Russolillo, G., & Meroni, G. (2008). MID1 mutations in patients with X-linked Opitz G/BBB syndrome. *Human Mutation*, 29(5), 584–594. <https://doi.org/10.1002/humu.20706>
- gnomAD, Genome Aggregation Database. (2021). <http://gnomad.broadinstitute.org>
- Huang, J., Rauscher, S., Nawrocki, G., Ran, T., Feig, M., de Groot, B. L., Grubmüller, H., & MacKerell, A. D. (2017). CHARMM36m: An improved force field for folded and intrinsically disordered proteins. *Nature Methods*, 14(1), 71–73. <https://doi.org/10.1038/nmeth.4067>
- Hüning, I., Kutsche, K., Rajaei, S., Erlandsson, A., Lovmar, L., Rundberg, J., & Stefanova, M. (2013). Exon 2 duplication of the MID1 gene in a patient with a mild phenotype of Opitz G/BBB syndrome. *European Journal of Medical Genetics*, 56(4), 188–191. <https://doi.org/10.1016/j.ejmg.2013.01.004>
- Jorgensen, W. L., Chandrasekhar, J., Madura, J. D., Impey, R. W., & Klein, M. L. (1983). Comparison of simple potential functions for simulating liquid water. *Journal of Chemical Physics*, 79, 926–935. <https://doi.org/10.1063/1.445869>
- Jumper, J., Evans, R., Pritzel, A., Green, T., Figurnov, M., Ronneberger, O., Tunyasuvunakool, K., Bates, R., Židek, A., Potapenko, A., Bridgland, A., Meyer, C., Kohl, S. A. A., Ballard, A. J., Cowie, A., Romera-Paredes, B., Nikolov, S., Jain, R., Adler, J., ... Hassabis, D. (2021). Highly accurate protein structure prediction with AlphaFold. *Nature*, 596(7873), 583–589. <https://doi.org/10.1038/s41586-021-03819-2>
- Liu, J., Prickett, T. D., Elliott, E., Meroni, G., & Brautigan, D. L. (2001). Phosphorylation and microtubule association of the Opitz syndrome protein mid-1 is regulated by protein phosphatase 2A via binding to the regulatory subunit alpha 4. *Proceedings of the National Academy of Sciences of the United States of America*, 98(12), 6650–6655. <https://doi.org/10.1073/pnas.111154698>
- Maia, N., Nabais Sá, M. J., Tkachenko, N., Soares, G., Marques, I., Rodrigues, B., Fortuna, A. M., Santos, R., de Brouwer, A. P. M., & Jorge, P. (2017). Two novel pathogenic MID1 variants and genotype-phenotype correlation reanalysis in X-linked Opitz G/BBB syndrome. *Molecular Syndromology*, 9(1), 45–51. <https://doi.org/10.1159/000479177>
- Massiah, M. A., Simmons, B. N., Short, K. M., & Cox, T. C. (2006). Solution structure of the RBCC/TRIM B-box1 domain of human MID1: B-box with a RING. *Journal of Molecular Biology*, 358(2), 532–545. <https://doi.org/10.1016/j.jmb.2006.02.009>
- Meroni, G. (1993). X-linked Opitz G/BBB syndrome. In M. P. Adam, H. H. Ardinger, R. A. Pagon, S. E. Wallace, L. J. H. Bean, G. Mirzaa, & A. Amemiya (Eds.), *GeneReviews*(®). University of Washington, Seattle Copyright © 1993-2021, University of Washington, Seattle. GeneReviews is a registered trademark of the University of Washington, Seattle. All rights reserved.
- Mnayer, L., Khuri, S., Merheby, H. A., Meroni, G., & Elsas, L. J. (2006). A structure-function study of MID1 mutations associated with a mild Opitz phenotype. *Molecular Genetics and Metabolism*, 87(3), 198–203. <https://doi.org/10.1016/j.ymgme.2005.10.014>
- Pinson, L., Augé, J., Audollent, S., Mattéi, G., Etchevers, H., Gigarel, N., Razavi, F., Lacombe, D., Odent, S., Le Merrer, M., Amiel, J., Munnich, A., Meroni, G., Lyonnet, S., Vekemans, M., & Attié-Bitach, T. (2004). Embryonic expression of the human MID1 gene and its mutations in Opitz syndrome. *Journal of Medical Genetics*, 41(5), 381–386. <https://doi.org/10.1136/jmg.2003.014829>
- Preiksaitiene, E., Krasovskaja, N., Utkus, A., Kasnauskiene, J., Meškienė, R., Paulauskiene, I., Valevičienė, N. R., & Kučinskis, V. (2015). R368X mutation in MID1 among recurrent mutations in patients with X-linked Opitz G/BBB syndrome. *Clinical Dysmorphology*, 24(1), 7–12. <https://doi.org/10.1097/mcd.000000000000059>
- Richards, S., Aziz, N., Bale, S., Bick, D., Das, S., Gastier-Foster, J., Grody, W. W., Hegde, M., Lyon, E., Spector, E., Voelkerding, K., Rehm, H. L., & ACMG Laboratory Quality Assurance Committee. (2015). Standards and guidelines for the interpretation of sequence variants: A joint consensus recommendation of the American College of Medical Genetics and Genomics and the Association for Molecular Pathology. *Genetics in Medicine*, 17(5), 405–424. <https://doi.org/10.1038/gim.2015.30>
- Ruiter, M., Kamsteeg, E. J., Meroni, G., & de Vries, B. B. A. (2010). A MID1 mutation associated with reduced penetrance of X-linked Opitz G/BBB syndrome. *Clinical Dysmorphology*, 19(4), 195–197. <https://doi.org/10.1097/MCD.0b013e32833dc5ee>
- Shaw, A., Longman, C., Irving, M., & Splitt, M. (2006). Neonatal teeth in X-linked Opitz (G/BBB) syndrome. *Clinical Dysmorphology*, 15(3), 185–186. <https://doi.org/10.1097/01.mcd.0000198931.09330.e8>
- Short, K. M., Hopwood, B., Yi, Z., & Cox, T. C. (2002). MID1 and MID2 homo- and heterodimerise to tether the rapamycin-sensitive PP2A regulatory subunit, alpha 4, to microtubules: Implications for the clinical variability of X-linked Opitz GBBB syndrome and other developmental disorders. *BMC Cell Biology*, 3, 1. <https://doi.org/10.1186/1471-2121-3-1>
- So, J., Suckow, V., Kijas, Z., Kalscheuer, V., Moser, B., Winter, J., Baars, M., Firth, H., Lunt, P., Hamel, B., Meinecke, P., Moraine, C., Odent, S., Schinzel, A., van der Smagt, J. J., Devriendt, K., Albrecht, B., Gillissen-Kaesbach, G., van der Burgt, I., ... Schweiger, S. (2005). Mild phenotypes in a series of patients with Opitz GBBB syndrome with MID1 mutations. *American Journal of Medical Genetics. Part A*, 132A(1), 1–7. <https://doi.org/10.1002/ajmg.a.30407>
- Tao, H., Simmons, B. N., Singireddy, S., Jakkidi, M., Short, K. M., Cox, T. C., & Massiah, M. A. (2008). Structure of the MID1 tandem B-boxes reveals an interaction reminiscent of intermolecular ring heterodimers. *Biochemistry*, 47(8), 2450–2457. <https://doi.org/10.1021/bi7018496>
- Taylor, A., Wilson, F., Hendrie, G. A., Allman-Farinelli, M., & Noakes, M. (2015). Feasibility of a healthy trolley index to assess dietary quality of the household food supply. *The British Journal of Nutrition*, 114(12), 2129–2137. <https://doi.org/10.1017/S0007114515003827>
- Trockenbacher, A., Suckow, V., Foerster, J., Winter, J., Krauss, S., Ropers, H. H., Schneider, R., & Schweiger, S. (2001). MID1, mutated in Opitz syndrome, encodes an ubiquitin ligase that targets phosphatase 2A for degradation. *Nature Genetics*, 29(3), 287–294. <https://doi.org/10.1038/ng762>

- Uziela, K., Menéndez Hurtado, D., Shu, N., Wallner, B., & Elofsson, A. (2017). ProQ3D: Improved model quality assessments using deep learning. *Bioinformatics*, 33(10), 1578–1580. <https://doi.org/10.1093/bioinformatics/btw819>
- Waterhouse, A., Bertoni, M., Bienert, S., Studer, G., Tauriello, G., Gumienny, R., Heer, F. T., de Beer, T. A. P., Rempfer, C., Bordoli, L., Lepore, R., & Schwede, T. (2018). SWISS-MODEL: Homology modelling of protein structures and complexes. *Nucleic Acids Research*, 46(W1), W296–W303. <https://doi.org/10.1093/nar/gky427>
- Wright, K. M., Du, H., Dagnachew, M., & Massiah, M. A. (2016). Solution structure of the microtubule-targeting COS domain of MID1. *The FEBS Journal*, 283(16), 3089–3102. <https://doi.org/10.1111/febs.13795>
- Zhang, X., Chen, Y., Zhao, S., Markljung, E., & Nordenskjöld, A. (2011). Hypospadias associated with hypertelorism, the mildest

phenotype of Opitz syndrome. *Journal of Human Genetics*, 56(5), 348–351. <https://doi.org/10.1038/jhg.2011.17>

How to cite this article: Perea-Cabrera, M., Granados-Riveron, J. T., Segura-Stanford, B., Moreno-Vargas, L. M., Prada-Gracia, D., Moran-Espinosa, M. C., Erdmenger, J., Diaz-Garcia, H., & Sánchez-Urbina, R. (2023). Opitz GBBB syndrome with total anomalous pulmonary venous connection: A new MID1 gene variant. *Molecular Genetics & Genomic Medicine*, 11, e2234. <https://doi.org/10.1002/mgg3.2234>